

Reliability of Islanded Microgrids with Stochastic Generation and Prioritized Load

Scott Kennedy, *Member IEEE*, Mirjana Milošević Marden, *Member IEEE*

Abstract—The potential to improve distribution system reliability is a primary motivation behind the development and deployment of microgrids. Previous studies have illustrated substantial reliability benefits of dispatchable distributed energy resources (DER). However, more analysis and new evaluation methodologies are needed for microgrids dominated by limited and stochastic distributed generation (SDG). The present paper introduces an evaluation methodology for islanded microgrids that realistically represents stochastic resources and explicitly examines the influence of supply-to-load correlation on reliability. Monte-Carlo simulation is used to model component failure and repair, while historical data is used for the stochastic resource. SDG output is allocated to loads based on a prioritized order that accounts for the dynamic reconfiguration of the microgrid in the case of a local fault. Voluntary load curtailment and its impact on reliability are also examined. Simulation results reveal that the priority order of a given load section on an islanded microgrid with limited SDG determines its dominant cause of interruption and has a major influence on reliability.

Index Terms—microgrids, reliability, load curtailment, islanding.

I. INTRODUCTION

INCREASED attention is currently being paid to microgrids as an alternative or complement to large centralized generation plants, especially to their potential role in increasing power system reliability while forgoing or delaying large investments in transmission capacity. A microgrid can be defined as a section of a distribution system that contains distributed energy resources (DER) and can be isolated (islanded) from the rest of the network in the event of an upstream fault. The ability to increase reliability for customers within a microgrid depends on the sufficiency of the DER and whether or not the local generation units can quickly recover or even ride-through a nearby fault.

In previous studies that have addressed and analyzed the reliability impacts of microgrids, the DER is usually considered to be a dispatchable resource [1-4], or is stochastic, but with sufficient energy storage to make it essentially dispatchable [5]. These studies have focused primarily on reliability impacts as a function of the DER size, location, and

operating strategy. There have been relatively fewer studies that have examined microgrids with purely stochastic DER, such as solar and wind [6, 7], even though this type of stochastic distributed generation (SDG) may become the most prevalent type of DER. Evaluating reliability improvements from stochastic and non-dispatchable resources is more challenging as there are multiple stochastic processes that need to be considered: the load, the power supply and the failure and repair of the different network components. In standard distribution system reliability studies, the failure and repair of the various components are frequently considered independent of each other and of the load [8, 9]. However, with a stochastic supply, preserving the correlation between the SDG output and the load becomes essential in accurately estimating reliability.

Another challenge in evaluating the reliability impacts of SDG on an islanded microgrid is the fact that their supply is limited. The available power at any point in time may not satisfy all loads and must be allocated according to some restoration priority. In addition, a failure of any section on an islanded microgrid may initiate a network reconfiguration, which will alter the connectivity between the loads and the SDGs. A load restoration order that is sensitive to the dynamic reconfiguration of the microgrid network must therefore be specified and included in the reliability evaluation.

One approach to handle network reconfiguration and prioritized load recovery has been proposed in [2]. This methodology utilizes a connection matrix to represent the state of the network given the failure of any single network section. The technique has been applied to a system with a photovoltaic (PV) source in [5], although, in this case, the DER is essentially dispatchable because sufficient energy storage is present to accommodate any variability in supply.

The present paper introduces a methodology to estimate the reliability impacts of SDG on an islanded microgrid, while explicitly considering the correlation between SDG output and the load. The model includes an extension of previous work on prioritized load recovery for microgrids with dynamic reconfiguration. The microgrids that are examined contain only capacity limited SDG; dispatchable DER are not included. When SDG output is insufficient to satisfy the total load, voluntary load curtailment is considered as a possible course of action. A load curtailment coefficient is defined to estimate the impact of voluntary load curtailment on the reliability indices. Reliability indices as a function of load curtailment and a section's rank in the restoration order are

This work was supported by the Masdar Institute of Science and Technology.

S. Kennedy is with the Masdar Institute of Science and Technology, Abu Dhabi, UAE (e-mail: skennedy@mist.ac.ae).

M. Milošević Marden is with the Massachusetts Institute of Technology, Cambridge, MA, USA (e-mail: mirjana@mit.edu).

examined in detail.

The following section introduces the microgrid representation as well as the modeling methodology. A case study is presented in section III. Simulation results and the calculation of reliability indices are presented in section IV, followed by conclusion in section V.

II. EVALUATION METHODOLOGY

A. Microgrid Representation

An islanded microgrid will be represented as an idealized network of loads, “sections”, and SDG units, as shown in Fig. 1 [2]. A section refers to a portion of the microgrid that can be isolated from the rest of the network if a failure occurs anywhere on that section. Section 3 is outlined as an example of a typical section with one load point and a line interconnecting two sections through circuit breakers, whereas section 1 shows a section that contains a SDG unit, a load point, and line.

All components (lines, buses, loads, etc.) that may make up a given section are aggregated into one component, i.e. only the failure and repair rates of the section as a whole are specified. Each SDG unit is also modeled as an individual and independent component, which can fail independently of the section to which it is connected. If desired, each section can be disaggregated further into its subcomponents, although for the purpose of the present paper this is not necessary.

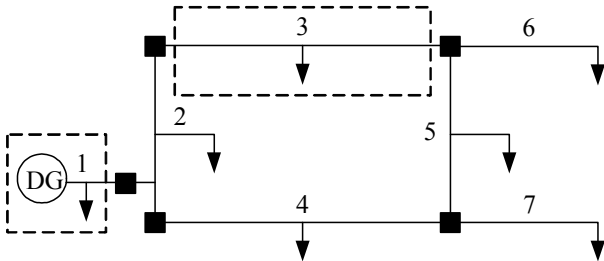


Fig. 1. Idealized microgrid with seven sections, seven load points, and one SDG unit. Two distinct sections are highlighted for illustrative purposes.

A loss of load for a given section can result from two causes. First, a section may fail and the microgrid would then change configuration, thereby causing some sections to lose their connectivity to the SDG source. Second, the limited and variable power output of the SDG units may not be sufficient to satisfy all loads. Whatever power that is available at a given time must be allocated to each section according to its specified priority. Sections with a lower priority would therefore suffer more frequent or more sustained outages.

B. Overall Model Flow

We propose a simulation-based approach for evaluating reliability whereby time series are generated for the energy resource availability (e.g. solar radiation or wind speed) at each SDG location, $ER_k(t)$, the load on each section, $L_i(t)$, the technical availability of each SDG unit, $SDG_k(t)$, and the technical availability of all network sections, $N_j(t)$. A flow chart illustrating the steps in the simulation model is shown in

Fig. 2. A description of each of these quantities and the different simulation approaches used for generating them are described in the next sections.

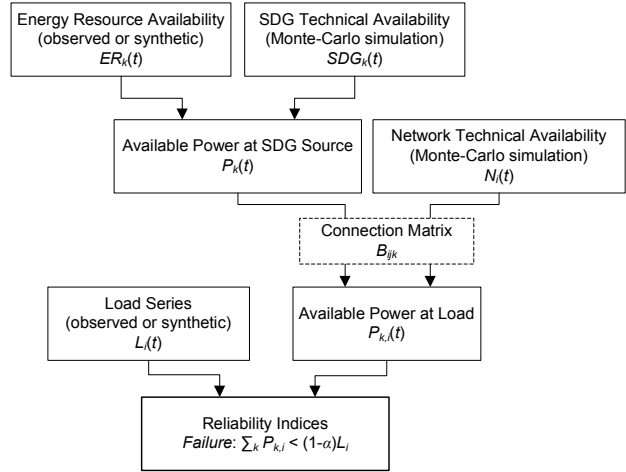


Fig. 2. Model flow for determining reliability indices.

C. Stochastic Processes for Energy Resource and Load, $ER_k(t)$ and $L_i(t)$

The simulation procedure for the load and the energy resource availability should realistically represent their time varying behavior and any correlation between them. Positive correlation between the energy resource and load will have a significant influence on microgrid reliability. However, this correlation is lost whenever time series values for the energy resource are generated independent of the load with commonly used non-sequential Monte-Carlo techniques [6] or first-order Markov processes [7]. It is therefore preferable to use either historical and simultaneous observations of load and energy resource data or to generate synthetic time series that preserve the autocorrelation of the original data [10].

When the SDG units are distributed spatially across the microgrid network, it is also important to consider the correlation of the energy resource across the different sites. Assuming that the random behavior of each source is independent from all others will likely underestimate the true variability of total power output [11], and potentially overestimate the reliability of the microgrid.

The energy resource data can be converted into SDG power output by multiplying the former by a fixed conversion efficiency (e.g. for PV source) or through interpolation of a standard power curve (e.g. for wind power), which relates the power in the resource to the electrical power output of the SDG.

D. Technical Availability of SDG and Network Sections, $SDG_k(t)$ and $N_j(t)$

The technical availability time series for the network sections and the SDG units can be generated using an event-based Monte-Carlo approach [9]. Independent probability distribution functions are assumed for each component, which implies that co-dependent failures of multiple sections or SDG units are not considered. It is further assumed that only one

network section can be down at a time. If co-dependent failures are neglected and the failure rate of a single network section is relatively low (~ 0.1 failure/year) and average repair rate is relatively short (~ 2 hr), the assumption of experiencing only one failure at a time for a small system is not very restrictive.

The technical availability of each SDG unit, $SDG_k(t)$, and network section, $N_i(t)$, can be expressed as a series of binary values (0, 1) that is generated by assuming some distribution function for the time to failure and time to repair for that component. Exponential distributions have been used for the present study and the average failure and repair rates are given later in the description of the case study.

The available SDG power at each source, $P_k(t)$, is the product of the energy resource availability, the conversion efficiency at that resource level, and the technical availability of the SDG unit,

$$P_k(t) = ER_k(t) \cdot f_{eff}(ER_k(t)) \cdot SDG_k(t), \quad (1)$$

where $f_{eff}(ER_k(t))$ is a general expression for the efficiency of converting the energy resource to electrical power output.

E. Connection Matrix, $B_{ijk}(t)$ and Prioritized Load Recovery

If a network section fails, some load points may no longer have access to the SDG units. To calculate the available power at each load point, it is therefore necessary to know the connectivity between all load points and all SDG units given the current state of the network. This task is accomplished using a connection matrix, B_{ijk} , that specifies whether a load point on section i is connected to SDG unit k , given that network section j is down [2]. The matrix also specifies the order by which each SDG unit should provide power for each section. The connection matrix is specified for a particular network *a priori* and does not need to be updated during the simulation.

For the example system in Fig. 1, a possible connection matrix with the sections numbered in terms of their priority would be,

$$B_{ijk} = \begin{bmatrix} 0 & 1 & 1 & 1 & 1 & 1 & 1 & 1 \\ 0 & 0 & 2 & 2 & 2 & 2 & 2 & 2 \\ 0 & 2 & 0 & 3 & 3 & 3 & 3 & 3 \\ 0 & 3 & 3 & 0 & 4 & 4 & 4 & 4 \\ 0 & 4 & 4 & 4 & 0 & 5 & 5 & 5 \\ 0 & 5 & 5 & 5 & 5 & 0 & 6 & 6 \\ 0 & 6 & 6 & 6 & 6 & 6 & 0 & 7 \end{bmatrix}. \quad (2)$$

A final eighth column is added to specify the priority order for a situation when all sections are operational. This extra column is only necessary when the SDG source is limited and cannot satisfy the combined load across all sections.

In this example, only the sections that have failed lose their connection to the SDG unit on section 1. However, it is straightforward to have a section lose connectivity due to failures on different section or to reorder the priority. The order shown in (2) is used simply to illustrate more clearly the

results in the following case study.

For a given point in time, the state of all sections is specified by the time series $N_i(t)$, with $i \in [1,7]$ for the example system. The available power $P_{k,i}(t)$ from SDG unit k at section i can be found by first allocating the power from SDG unit k to all sections with a higher priority than i , and then using the remainder to serve the load on section i . This procedure is accomplished using the recursive relationship between the available SDG power and the load on each section developed in [2] and reproduced below,

$$\begin{cases} L_{k,i,j}(t) = L_{k-1,i,j}(t) - P_{k,i',j}(t), & L_{k-1,i,j}(t) > P_{k,i',j}(t) \\ L_{k,i,j}(t) = 0, & \text{otherwise} \end{cases} \quad (3)$$

$$\begin{cases} P_{k,i,j}(t) = P_{k,i',j}(t) - L_{k-1,i,j}(t), & P_{k,i',j}(t) > L_{k-1,i,j}(t) \\ P_{k,i,j}(t) = 0, & \text{otherwise} \end{cases} \quad (4)$$

where $L_{k,i,j}(t)$ is the remaining load on section i after the power from SDG units 1 through k have been allocated to all sections, $P_{k,i,j}(t)$ is the remaining available power of SDG unit k after this unit has been used to recover all sections up to i in priority order, i' refers to the section prior to i in priority order, and j refers to the section that is currently down (for all sections up, $j=0$).

The initial values for (3) and (4), $L_{0,i,j}(t)$ and $P_{k,0,j}(t)$, are set to the load on each section, $L_i(t)$, and total available power, $P_k(t)$, respectively.

F. Calculation of Reliability Indices

With a simulation based approach, it is possible to generate a rich set of output data from which average reliability indices and their distributions can be examined. In the present study, the reliability indices of interest include the energy not served (ENS), the unavailability (U), the interruption frequency, and the repair time. For the former two indices, the annual totals are examined, whereas for the latter two, both empirical distributions and annual averages will be presented.

In the present study, an interruption is defined to occur whenever the available power for a given section drops below the load at that section *after* subtracting all voluntary curtailment. Voluntary curtailment is expressed in terms of a load curtailment coefficient, α , that is a fixed percentage of the instantaneous load. An interruption can therefore be defined using either of the two equivalent expressions below,

$$\sum_k P_{k,i}(t) < (1 - \alpha) L_i(t), \quad (5)$$

$$L_{K,i,j}(t) > \alpha L_i(t), \quad (6)$$

where K is the last SDG unit in the iteration shown in (3) and (4). Defining an interruption only after voluntary curtailment is useful as it allows for a simple assessment of the benefits of partial load curtailment (or demand response) on the reliability indices.

III. CASE STUDY

A. Test System

The sample system with 7 sections and one SDG unit that is shown in Fig. 1 will be used for the case study. This test system is similar in structure to the system presented in [5], except that the section numbers have been reordered in terms of their priority; section 1 is supplied first by the SDG, followed by section 2, and so on. The SDG unit is modeled in this case as a PV array.

B. Photovoltaic Output and Load Data

A time series for the PV output in section 1 is generated from historical five minute averaged solar irradiation data that was obtained from the CONFRRM monitoring program at Elizabeth City State University, North Carolina [12]. Solar irradiation data covering 12 months in 2007 is converted to power output assuming a conversion efficiency of 15% with the panels installed in a flat orientation. The PV installation is assumed to have an average of 1 failure per year and an average repair time of 168 hours, as shown in Table I.

TABLE I
FAILURE AND REPAIR TIME

Unit	Failure Rate (f/year)	Repair time(h)
PV array	1	168
Section	0.1	2

A deterministic load model was chosen in order to more clearly observe the influence of the stochastic nature of PV output on microgrid reliability. A simple sine curve is used for the load on each section. By representing the load as a sinusoid (as opposed to a fixed load), it is possible to shift the phase (ϕ) and examine the influence that the correlation between PV output and load has on the reliability indices,

$$L_i(t) = L_o(1 + \sin[\pi t/12 - \phi]) + L_{min} . \quad (7)$$

The magnitude of the load on each section is scaled such that the sum of loads over all sections has a minimum value equal to 25% and a maximum value equal to 80% of the maximum PV output.

All sections are assumed to have equivalent failure and repair rates. Different rates can be assigned according to each section's length or the number of its subcomponents, however with different values for each section, the influence of PV variability and load priority on the reliability indices become less clear. It was therefore decided to keep the failure and repair rates the same for all sections.

The power output for 120 kW of installed PV capacity for all of 2007 and a typical week in mid-July are shown in Fig. 3. From the top plot, a seasonal trend is clearly evident with the average daily peak output during the summer almost twice the output during the winter months. The load curve, shown in light gray, is assumed to be consistent across the year. The low PV output in the winter months will result in either more frequent or more sustained load interruptions as will be explained later. The gaps in the PV output correspond to two failures during the course of one year. The daily PV output

shown in the bottom plot shows a significant variability from day to day, with the last day in the series having no output due to a failure of the PV system.

The load time series for a single section and the combined total for all seven sections is also shown in the bottom plot of Fig. 3. The highest priority section would receive power through most of the day, while the lowest priority section would only receive power during the peak daylight hours during the summer months. For the present case, the peak values for load and PV output are coincident. This will be changed later by adjusting the value of ϕ in (7).

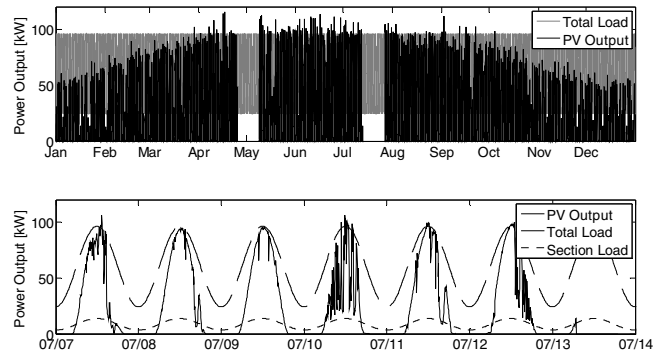


Fig. 3. PV power output and total load on all sections shown for one year and a typical week in mid-July. (maybe to make the font size of the figure bigger)

IV. SIMULATION RESULTS

A. Reliability Indices for Different Sections

Reliability indices have been calculated for each section over a 10 year time horizon. Solar irradiation data for a 1 year period was repeated across the 10 years, while the failure and repair rates of the PV installation and each section were simulated for the full 10 years. The results for each section, which include energy not served (ENS), unavailability (U), average interruption frequency index (AIFI), and average interruption duration index (AIDI), are shown in Table II. The ENS is expressed as a percentage of the total energy demand. For all cases, the load curtailment coefficient was set to zero.

TABLE II
RELIABILITY INDICES BY SECTION

Section Number	ENS (%)	U (hr/yr)	AIFI (f/yr)	AIDI (hr)
1	41.41	5,573	746.2	7.47
2	53.22	6,262	1,136	5.51
3	62.63	6,809	1,429	4.76
4	71.45	7,378	1,455	5.07
5	80.30	7,861	1,201	6.45
6	87.95	8,293	894.0	9.07
7	95.08	8,664	349.3	24.2

ENS is expressed as a percentage of the total energy demand.

The trend in the first two columns is as expected; the lower the priority of the section, the higher the values of ENS and U. The values are relatively high (i.e. low reliability) because the evaluation has been performed for an islanded microgrid with PV as the only available source. In a broader context, the values could be multiplied by the probability of islanding if the microgrid regularly operates with a connection to an upstream network.

For the second two columns, two interesting observations can be made. First, there is an inverse relation between the frequency and duration of interruptions; and second, the interruption frequency rises (duration decreases) moving halfway down the priority order, but then the trend reverses and the frequency decreases (duration increases). The reason for the non-monotonic relation between reliability and load priority can be explained by the dominant type of interruption for each section. Low priority sections are normally supplied with power for only a brief period during the middle of the day. Interruptions therefore typically last around 24 hours and occur roughly once per day. The AIDI value for section 7 is actually higher than 24 hours due to the low resource in winter months when an interruption can last several days. The mid-priority sections are supplied by the PV array for a longer period during the day, but will be dropped under cloudy conditions when output is reduced. These sections therefore have a higher failure frequency and lower failure duration. The high priority sections are also supplied over most of the day, but they continue to receive power when cloudy conditions cause a partial reduction in output. Interruptions for high priority sections are typically due to nighttime periods or extremely cloudy conditions, occurring roughly twice per day, with an average duration of around 7.5 hours.

One general conclusion from these results is that increased access to an intermittent PV generator, when access is previously very limited, can potentially *increase* interruption frequency due to the inherently variable nature of the power supply.

B. Duration of Periods without Failure

Empirical distributions for the duration of periods without any failure can be compared across the different sections. From these distributions, the nature of the failures for the different sections can be inferred. In Fig. 4, histograms are shown for a sample of operating periods for sections 1, 4 and 7 over a 10 year time horizon.

The highest priority section shown in Fig. 4(a) has a relatively higher number of long operating periods, illustrating that this section can remain energized for periods in excess of 12 hours. As the section priority decreases (Fig. 4(b,c)), the duration of sustained operating periods falls, supporting the conclusion that the limited output is insufficient to serve lower priority loads over all daylight hours.

C. Effect of Load Curtailment on Reliability

The load curtailment coefficient, α , quantifies the portion of load that will be voluntarily curtailed before registering an interruption. Fig. 5 and Fig. 6 show the impact of load curtailment on the values of ENS and U . As α increases, the value of ENS is significantly reduced, as there is less load subject to involuntary curtailment. However, for the unavailability, U , the value of α has a much smaller effect as shown in Fig. 6. Voluntary load curtailment in this case does not significantly reduce the total time of interruptions, but only reduces the amount of lost load.

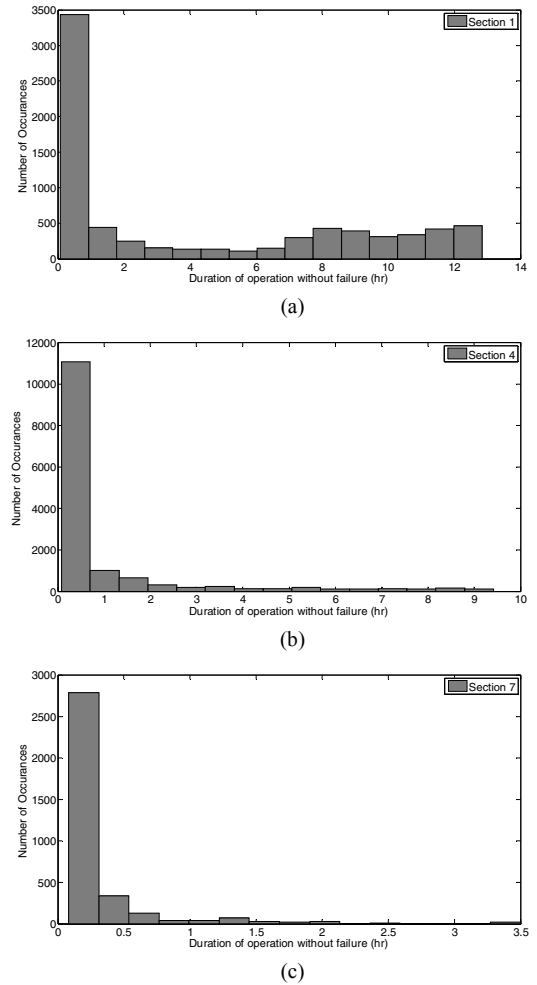


Fig. 4. Histograms for the duration of periods without failure for sections with high priority (a), medium priority (b), and low priority (c).

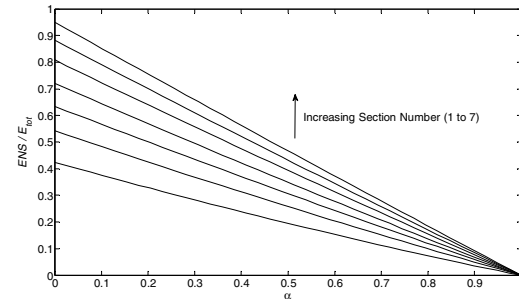


Fig. 5. Increasing the portion of load that can be curtailed reduces the values for ENS on all sections.

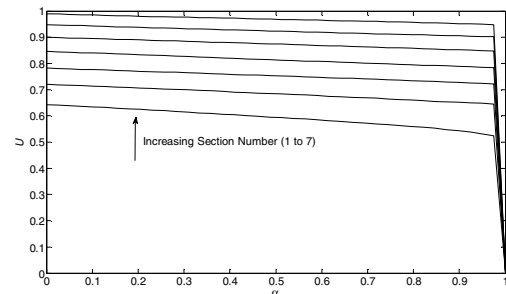


Fig. 6. Increasing the load curtailment coefficient has only a small affect on the unavailability due to interruptions occurring at night.

Voluntary load curtailment has a more subtle impact on the average frequency and duration of interruptions, as can be seen in Fig. 7 and Fig. 8. By increasing load curtailment for a high priority section, the average failure frequency (AIFI) will drop while the average failure duration (AIDI) will increase. The opposite trend is evident for the low priority sections. The mid-priority sections show little sensitivity to load curtailment (in terms of the values of AIFI and AIDI).

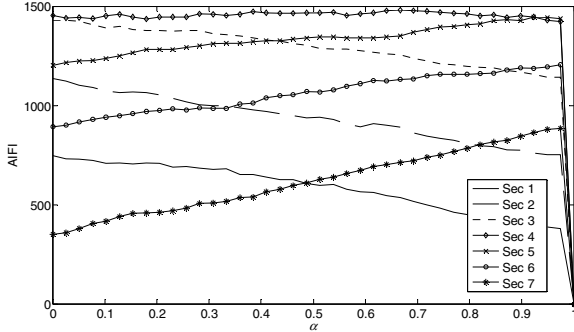


Fig. 7. Increasing voluntary load curtailment and its impact on failure frequency.

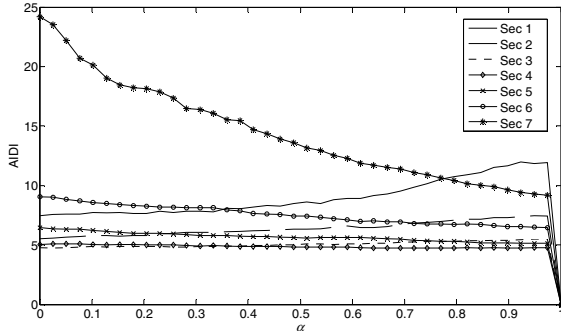


Fig. 8. Increasing voluntary load curtailment and its impact on failure duration.

The reason for the different impact of load curtailment on the different sections is explained as follows. For the high priority sections, increased load curtailment reduces the number of interruptions due to the occasional extreme cloudy condition, but can do nothing for nighttime interruptions. The number of short duration interruptions is therefore reduced, which decreases the value of AIFI and increases AIDI. For the low priority sections, on the other hand, an increase in load curtailment increases number of daylight supply hours, thereby increasing the number of short interruptions from routine cloudy conditions. This effect increases the value of AIFI and reduces AIDI. For the mid-priority sections, increasing load curtailment does not change the dominant type of interruption and the AIFI and AIDI remain relatively unaffected.

These results indicate that the effects of increasing load curtailment (or equivalently, increasing supply capacity) on AIFI and AIDI depend to a great extent on the dominate type of interruptions experienced by a particular section. Increased

vulnerability to interruptions resulting from cloudy conditions tends to increase AIFI and reduce AIDI, while reduced vulnerability to cloudy conditions leads to the opposite effect.

D. Influence of Correlation Coefficient on Reliability

The correlation between the load, $L_i(t)$, and the SDG power supply $P_k(t)$, can be measured by a correlation coefficient, ρ_{DG-L} , that is the statistical correlation between these two time series. The value of ρ_{DG-L} can be adjusted by altering the phase angle, ϕ , in (7). The relationship between phase angle and the correlation coefficient for the data used in this study is shown in Fig. 9.

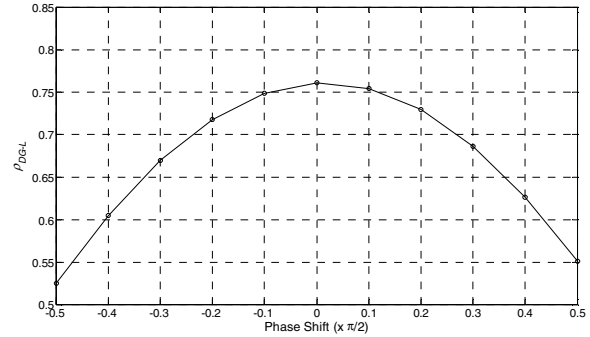


Fig. 9. Relationship between the correlation coefficient and the phase angle ϕ in the load model.

Identical reliability evaluations have been conducted using load series with different values of ρ_{DG-L} . The results show that the section priority again has a significant influence. Fig. 10 shows that the high priority loads have a lower ENS value when the load-to-supply correlation increases, as would be expected. However, for the low priority loads, the opposite trend is evident; a higher correlation leads to a larger amount of unmet load.

In the case of U , Fig. 11 reveals that the number of hours of interruption is relatively insensitive to the correlation coefficient for the high priority loads, but for low priority loads, the value of U increases with a rising correlation. In effect, an increase in the load-to-supply correlation worsens the reliability for the low priority sections. This result can be explained by examining the load and PV output curves in Fig. 3. When the correlation between load and supply is high, the bulk of the PV output is supplied to the high and mid-priority loads. However, when the correlation decreases, the load and supply peak are no longer coincident. In this case the PV supply peak occurs at a time of lower *total* load. A higher share of the output can then be allocated to the low priority sections.

Increasing the load-to-supply correlation for a microgrid with SDG can potentially worsen reliability for certain sections, since the new correlation will result in a re-allocation of the limited power output across the different sections.

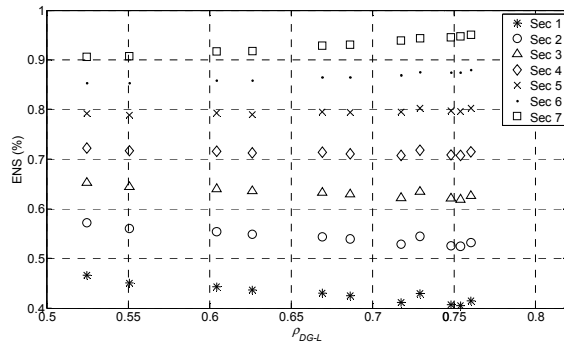


Fig. 10. Variation of ENS with correlation between load and PV output for different sections.

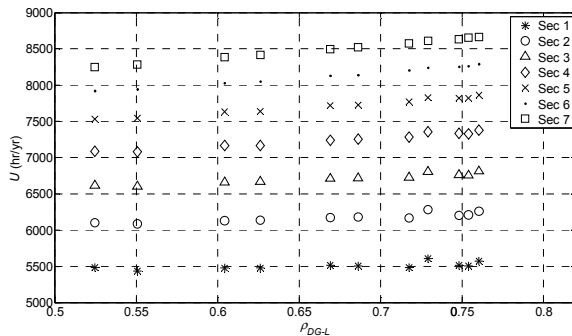


Fig. 11. Variation of U with correlation between load and PV output for different sections.

V. CONCLUSION

This paper has presented a new methodology for evaluating the reliability indices for an islanded microgrid with purely stochastic distributed generation. The method extends previous work on allocating limited output from distributed generation sources according to a prioritized load restoration order. Interruptions have been defined with respect to a voluntary load curtailment coefficient to estimate the impact of load curtailment on reliability indices.

Simulation results for a microgrid with a PV source have shown that the type of interruption (e.g. nighttime, routine clouds, extremely cloudy) varies according to a sections' rank in the restoration order. The dominant interruption type plays a significant role in determining the reliability indices and the sensitivity of the indices to load curtailment and the load-to-supply correlation. Further work is needed to explore the reliability of islanded microgrids with a greater variety of both stochastic and dispatchable DER.

REFERENCES

- [1] I.-S. Bae, J.-O. Kim, J.-C. Kim, and C. Singh, "Optimal operating strategy for distributed generation considering hourly reliability worth," *Power Systems, IEEE Transactions on*, vol. 19, pp. 287-292, 2004.
- [2] I. S. Bae and J. O. Kim, "Reliability Evaluation of Distributed Generation Based on Operation Mode," *Power Systems, IEEE Transactions on*, vol. 22, pp. 785-790, 2007.
- [3] M. H. J. Bollen, Y. Sun, and G. W. Ault, "Reliability of distribution networks with DER including intentional islanding," in *Future Power Systems, 2005 International Conference on*, 2005, p. 6 pp.
- [4] Y. Sun, M. H. J. Bollen, and G. W. Ault, "Probabilistic Reliability Evaluation for Distribution Systems with DER and Microgrids," in

Probabilistic Methods Applied to Power Systems, 2006. PMAPS 2006. International Conference on, 2006, pp. 1-8.

- [5] I.-S. Bae and J. O. Kim, "Reliability Evaluation of Customers in a Microgrid," *Power Systems, IEEE Transactions on*, vol. 23, pp. 1416-1422, 2008.
- [6] Y. G. Hegazy, M. M. A. Salama, and A. Y. Chikhani, "Adequacy assessment of distributed generation systems using Monte Carlo Simulation," *Power Systems, IEEE Transactions on*, vol. 18, pp. 48-52, 2003.
- [7] R. Yokoyama, T. Niimura, and N. Saito, "Modeling and evaluation of supply reliability of microgrids including PV and wind power," in *Power and Energy Society General Meeting - Conversion and Delivery of Electrical Energy in the 21st Century, 2008 IEEE*, 2008, pp. 1-5.
- [8] R. Billinton and R. N. Allan, *Reliability evaluation of power systems*, 2nd ed. ed. New York ; London: Plenum Press, 1996.
- [9] R. Billinton and W. Li, *Reliability assessment of electric power systems using Monte Carlo methods*. New York ; London: Plenum Press, 1994.
- [10] S. Kennedy and P. Rogers, "A Probabilistic Model for Simulating Long-Term Wind-Power Output," *Wind Engineering*, pp. 167-181, 2003.
- [11] G. Papaefthymiou, P. H. Schavemaker, L. van der Sluis, W. L. Kling, D. Kurowicka, and R. M. Cooke, "Integration of stochastic generation in power systems," *International Journal of Electrical Power & Energy Systems*, vol. 28, pp. 655-667, 2006.
- [12] NREL, "Cooperative Networks For Renewable Resource Measurements - CONFRRM." vol. 2008 Golden: National Renewable Energy Lab, 2008.



Scott W. Kennedy (M'2008) became a Member of IEEE in 2008. He received a PhD in Engineering Sciences and an S.M in Applied Math from Harvard University, Cambridge, MA in 2003.

He is an Associate Professor at the Masdar Institute of Science and Technology in Abu Dhabi, UAE. His current research interests include the integration of renewable energy sources into power networks, with an emphasis on the interactions between power markets and power system operations.



Mirjana Milošević Marden (M'2004) was born in Novi Sad, Serbia. She obtained her Dipl.Ing. degree from the University of Novi Sad in 1999, MSc. degree in 2002 from Northeastern University, Boston, MA and Ph.D. degree in 2007 from Swiss Federal Institute of Technology (ETH), Zurich. She is currently employed as a Postdoctoral Associate at Massachusetts Institute of Technology (MIT) in Cambridge, MA. Her research interests concern integration of renewable energy sources into power systems, microgrid analysis

and control.